# Real-Time Dynamics in Quantum-Impurity Systems: A Time-Dependent Numerical Renormalization-Group Approach

Frithjof B. Anders[1] and Avraham Schiller[2]

[1]*Department of Physics, Universität Bremen, P.O. Box 330 440, D-28334 Bremen, Germany*

[2]*Racah Institute of Physics, The Hebrew University, Jerusalem 91904, Israel*

(Received 29 April 2005; published 31 October 2005)

We develop a general approach to the nonequilibrium dynamics of quantum-impurity systems for arbitrary coupling strength. The numerical renormalization group is used to generate a complete basis set necessary for the correct description of the time evolution. We benchmark our method with the exact analytical solution for the resonant-level model. As a first application, we investigate the equilibration of an ultrasmall quantum dot subject to a sudden change of gate voltage and external magnetic field. Two distinct relaxation times are identified for the spin and charge dynamics.

DOI: 10.1103/PhysRevLett.95.196801 PACS numbers: 73.63.Kv, 03.65.Yz, 73.21.La, 76.20.+q

*Introduction.*—The investigation of real-time dynamics in quantum-impurity systems (QIS) is of prime importance for our understanding of dissipation and decoherence in qubits and electronic transport through nanodevices. Such systems consist of a mesoscopic subsystem or device, interacting with an infinitely large environment of noninteracting particles. Typical examples are quantum dots, qubits, or biological donor-acceptor molecules. These are usually modeled either by a spin-Bose model, where a two-level system or qubit is interacting with a bosonic bath [1], or by a set of atomic orbitals coupled to electronic leads, as in ultrasmall quantum dots and single-electron transistors [2]. The practical importance of real-time dynamics in quantum dots for quantum computing was recently emphasized by Elzerman *et al.* [3], who used the temporal response to gate-voltage pulses for a single-shot read out of the spin configuration of a quantum dot in a finite magnetic field.

In contrast to equilibrium conditions, the understanding of the real-time evolution of many-particle quantum systems is still in its infancy. Over the past 40 years, the Keldysh technique [4] has proven to be the most successful approach to nonequilibrium (NEQ) dynamics, as it furbishes a perturbative expansion of the density operator. In general, however, perturbation theory fails in QIS due to the infrared divergences caused by degeneracies on the impurity. Recently, there has been significant progress in extending the density-matrix renormalization-group (DMRG) to time-dependent 1D quantum systems [5–8]. The so-called TD-DMRG works well for finite-size systems and short times, but has an accumulated error proportional to the time elapsed. This makes the TD-DMRG unsuitable at present for tackling long time scales, most notably the exponentially long time associated with the development of the Kondo effect [9].

In this Letter, we develop an alternative approach to the real-time dynamics of QIS based on Wilson's numerical renormalization-group (NRG) method [10]. The NRG is a very powerful and accurate tool for calculating equilibrium properties of arbitrarily complex quantum impurities. We extend the approach to a certain class of time-dependent problems where a sudden perturbation, e.g., a gate-voltage pulse [3], is applied to the impurity at time $t = 0$. An earlier attempt [11] at a time-dependent NRG (TD-NRG) was faced with conceptual problems of how to adequately couple the low- and high-energy scales. Here we resolve these problems by combining the NRG with Feynman's concept of a reduced density matrix [12,13], and by implementing a suitable resummation procedure for tracking all states that contribute to the time evolution of the system. We establish the accuracy of our approach by comparison to the exact analytical solution of the resonant-level model, and apply it to the single impurity Anderson model (SIAM). Two distinct time scales are found for the spin and charge dynamics in the SIAM. The process of spin relaxation is shown to be sensitive to the initial conditions imposed on the system.

*Formulation.*—As our approach applies to arbitrary QIS, we first formulate it in general terms before turning to concrete examples. The Hamiltonian of QIS is generally given by $\mathcal{H}^i = \mathcal{H}_{\rm bath} + \mathcal{H}_{\rm imp} + \mathcal{H}_{\rm mix}$, where $\mathcal{H}_{\rm bath}$ models the continuous bath, $\mathcal{H}_{\rm imp}$ represents the decoupled impurity, and $\mathcal{H}_{\rm mix}$ describes the coupling between the two subsystems. The entire system is assumed to be in thermal equilibrium for $t < 0$, at which point a sudden perturbation $\Delta\mathcal{H}$ is switched on: $\mathcal{H}(t > 0) = \mathcal{H}^i + \Delta\mathcal{H} \equiv \mathcal{H}^f$. For $t > 0$, the density-matrix operator evolves according to $\hat{\rho}(t > 0) = e^{-{\rm i}t\mathcal{H}^f}\hat{\rho}_{\rm eq}e^{{\rm i}t\mathcal{H}^f}$, where $\hat{\rho}_{\rm eq} = e^{-\beta\mathcal{H}^i}/{\rm Tr}\{e^{-\beta\mathcal{H}^i}\}$.

The key ingredient in the NRG is a logarithmic discretization of the continuous bath, controlled by the parameter $\Lambda > 1$ [10]. The Hamiltonian is mapped onto a semi-infinite chain, where the $N$th link represents an exponentially decreasing energy scale $D_N \sim \Lambda^{-N/2}$ [10]. Using this hierarchy of scales, the sequence of finite-size Hamiltonians $\mathcal{H}_N$ for the $N$-site chain is solved iteratively, truncating the high-energy states at the conclusion of each step so as to maintain a manageable number

 

of states. The reduced basis set of $\mathcal{H}_N$ so obtained is expected to faithfully describe the spectrum of the full Hamiltonian on a scale of $D_N$, corresponding to the temperature $T_N \sim D_N$ [10].

Out of equilibrium, one can no longer settle with the reduced basis set of $\mathcal{H}_N^f$ at temperature $T_N$, as the NEQ dynamics involves all energy scales exceeding $T_N$. A complete basis set of the Fock space $\mathcal{F}_N$ of $\mathcal{H}_N$ is required. One possible choice of a complete basis set is given by $\mathcal{F}_N = \{|l, e; m\rangle_{\rm dis}\}$, where $l$ labels the NRG eigenstates of $\mathcal{H}_m^f$ *discarded* at iteration $m = 1, \ldots, N$, and $e$ is a tuple of quantum numbers labeling the "environment" degrees of freedom on the remaining chain tail $R_{m,N}$, see Fig. 1. For $m = N$, all NRG eigenstates are considered discarded. Restricting attention to local operators $\hat{O}$ which do not act on the environment degrees of freedom, the time evolution of $\langle\hat{O}\rangle$ is formally given by

$$\langle\hat{O}\rangle(t) = \sum_{m,m'}\sum_{l,l',e,e'} {}_{\rm dis}\langle l, e; m|\hat{O}|l', e'; m'\rangle_{\rm dis} \times {}_{\rm dis}\langle l', e'; m'|e^{-i\mathcal{H}_N^f t}\hat{\rho}_{\rm eq}e^{i\mathcal{H}_N^f t}|l, e; m\rangle_{\rm dis}. \quad (1)$$

The sum over $m$, $m'$ in Eq. (1) divides into three parts: $m > m'$, $m = m'$, and $m < m'$. Consider $m < m'$. Introducing the states $\{|l, e; m\rangle_{kp}\}$, where $l$ now labels the *retained* NRG eigenstates of $\mathcal{H}_m^f$ and $e$ records the environment degrees of freedom, one has the identity

$$\sum_{\substack{m',l',e'\\(m'>m)}} |l', e'; m'\rangle_{\rm dis}\ {}_{\rm dis}\langle l', e'; m'| = \sum_{l,e}|l, e; m\rangle_{kp}\ {}_{kp}\langle l, e; m|. \quad (2)$$

A similar identity applies to $m' < m$ upon interchanging the roles of $m$ and $m'$. Inserting Eq. (2) and its $m \leftrightarrow m'$ counterpart into Eq. (1) one obtains

$$\langle\hat{O}\rangle(t) = \sum_{m=0}^{N}\sum_{r,s}^{\rm trun} e^{i(E_r^m - E_s^m)t}O_{r,s}^m\rho_{s,r}^{\rm red}(m), \quad (3)$$

where $O_{r,s}^m = \langle r, e; m|\hat{O}|s, e; m\rangle$ is independent of $e$, and $\rho_{s,r}^{\rm red}$ is the *reduced density matrix* [12,13]

$$\rho_{s,r}^{\rm red}(m) = \sum_e \langle s, e; m|\hat{\rho}_{\rm eq}|r, e; m\rangle. \quad (4)$$

Here we have used the conventional NRG approximation $\mathcal{H}_N^f|l, e; m\rangle \approx E_l^m|l, e; m\rangle$, where $E_l^m$ is the NRG eigenenergy of $\mathcal{H}_m^f$ corresponding to the eigenstate $l$ [10]. The restricted sum $\sum_{r,s}^{\rm trun}$ in Eq. (3) implies that at least one of the states $r$ and $s$ is discarded at iteration $m$.

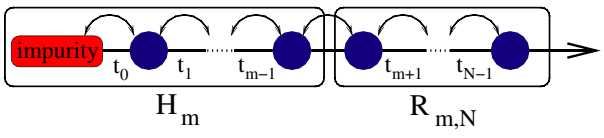


FIG. 1 (color online). The full NRG chain of length $N$ is divided into a subchain of length $m$ and the environment $R_{m,N}$.

Equation (3) is one of the central results of this Letter. In contrast to the TD-DMRG [5–8] and a previous attempt at a time-dependent NRG [11], all states of the finite-size Fock space are retained, and all energy scales are explicitly taken into account. No basis set reduction is imposed. To mimic the relaxation in an infinite-size system we (i) average Eq. (3) over $N_z$ different realizations of the NRG discretization using Oliveira's $z$ trick [14], and (ii) introduce a scale-dependent damping factor,

$$e^{i(E_r^m - E_s^m)t} \to e^{i(E_r^m - E_s^m)t}e^{-\alpha D_m t}, \quad (5)$$

for all $E_r^m \neq E_s^m$ in Eq. (3). Here $\alpha$ is an order 1 constant, representing a Lorentzian broadening of the NRG levels.

*Algorithm.*—To implement the TD-NRG at temperature $T$, one first selects a chain length $N$ such that $T \approx T_N$. Two simultaneous NRG runs are then performed, one for $\mathcal{H}^i$ and another for $\mathcal{H}^f$, to obtain (i) the equilibrium density matrix $\hat{\rho}_{\rm eq}$, (ii) the NRG eigenenergies and eigenstates of $\mathcal{H}^f$ and $\mathcal{H}^i$ up to iteration $N$, and (iii) the overlap matrices $S_{r,r'}(m)$ between the eigenstates of $\mathcal{H}^i$ and $\mathcal{H}^f$ at each iteration $m \leq N$. Using a recursion relation $\rho^{\rm red}(m) \to \rho^{\rm red}(m-1)$, the reduced density matrix of Eq. (4) is evaluated with respect to the NRG eigenstates of $\mathcal{H}^i$, and then rotated to the NRG eigenstates of $\mathcal{H}^f$ using the overlap matrices $S_{r,r'}(m)$. The recursion relation for $\rho^{\rm red}(m-1)$ relies on the fact that $\hat{\rho}_{\rm eq}$ is determined exclusively by the last NRG iteration $N$ [10]. Hence only the retained eigenstates of $\mathcal{H}_m^i$ contribute to the sum over $e$ in Eq. (4). The expectation value $\langle\hat{O}\rangle(t)$ follows from evaluation of Eq. (3).

*Benchmark.*—As a critical test of our method, we first apply it to the resonant-level model (RLM), describing the hybridization of a localized level $d^\dagger$ with a band of spinless conduction electrons $c_k^\dagger$:

$$\mathcal{H} = \sum_k \varepsilon_k c_k^\dagger c_k + E_d(t)d^\dagger d + V\sum_k\{d^\dagger c_k + c_k^\dagger d\}. \quad (6)$$

Choosing $\hat{n}_d = d^\dagger d$ as the observable $\hat{O}$, we consider a stepwise change in the energy of the level: $E_d(t) = \theta(-t)E_d^0 + \theta(t)E_d^1$. In the wideband limit, $n_d(t) = \langle\hat{n}_d\rangle(t)$ can be solved exactly in closed analytical form using the Keldysh formalism. For $T = 0$, the analytic solution features an exponential decay from the initial equilibrium occupancy of $\mathcal{H}^i$ to the new equilibrium occupancy of $\mathcal{H}^f$ with two decay rates $\Gamma$ and $2\Gamma$. Terms decaying at rate $\Gamma$ show an additional modulation of frequency $|E_d^1|$ [15]. Here $\Gamma = \pi\rho_0 V^2$ is the hybridization width, $\rho_0$ being the conduction-electron density of states at the Fermi energy.

Figure 2 shows a comparison of the TD-NRG with the exact analytical solution for $n_d(t)$, in response to a sudden change in the energy of the level from $E_d^0 = 0$ to $E_d^1 \neq 0$. Here we have used a symmetric box density of states $\rho(\varepsilon) = \rho_0\theta(D - |\varepsilon|)$ for the TD-NRG [10], and averaged over $N_z = 32$ equally spaced values of $z$ [14]. No damping

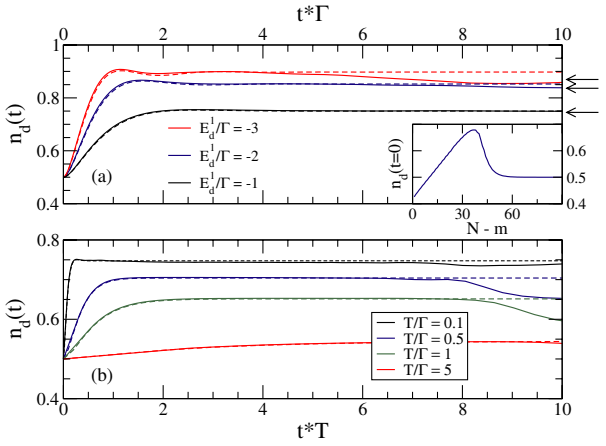


FIG. 2 (color online). Time-dependent occupancy of the RLM for (a) $E_d^0 = 0$, $T \to 0$ and three different values of $E_d^1/\Gamma = -1, -2, -3$, and (b) $E_d^0 = 0$, $E_d^1 = -\Gamma$ and four different temperatures $T/\Gamma = 0.1, 0.5, 1, 5$. Solid lines are the results of the TD-NRG with $\Lambda = 1.3$, $D/\Gamma = 500$, $N_z = 32$, $\alpha = 0$ (no damping factor) and $N_s = 1000$ states retained. Dashed lines are the exact solution in the wideband limit. Right arrows mark the saturated NRG occupancies for $\alpha > 0$. Inset to (a): Progressive calculation of $n_d(0)$ as a function of the number of backward iterations $N - m$, for $E_d^1 = -2\Gamma$.

factor was introduced. To facilitate comparison with the wideband limit, a large bandwidth $D/\Gamma = 500$ was used.

As seen in Fig. 2(a), the TD-NRG accurately reproduces the exact $T = 0$ solution *on all time scales* up to moderately large $E_d^1$. For $E_d^1 = -\Gamma$, the maximal error is less than 1%. For $E_d^1 = -2\Gamma$ it is less than 2.5%. The short-time behavior is well described by the TD-NRG for all $E_d^1$. In particular, $n_d(t \to 0^+)$ coincides with the initial equilibrium NRG occupancy of $\mathcal{H}^i$ independent of $E_d^0$ and $E_d^1$. As demonstrated in the inset to Fig. 2(a), summation over the states of all NRG iterations is essential for recovering $n_d(0)$. One cannot settle with just a single NRG iteration as in the equilibrium case.

Remarkably, the TD-NRG retains the same accuracy in Fig. 2(a) up to arbitrarily long times. Deviations from the new equilibrium occupancy of $\mathcal{H}^f$ are only slight at large $t$, and are further reduced by decreasing $\Lambda$ due to elongation of the effective chain length corresponding to the energy scale $E_d^1$. The long-time deviations in $n_d(t)$ stem from a difference between the time-evolved density matrix in a finite-size system and the equilibrium density matrix $\hat{\rho} \propto e^{-\beta \mathcal{H}^f}$, approached only for $\Lambda \to 1^+$.

The TD-NRG can also be applied to finite temperatures, see Fig. 2(b). For moderate $E_d^1$, there is excellent agreement with the exact curves up to $t$ several times larger than $1/T$, at which point finite-size oscillations develop. The latter oscillations are greatly reduced by averaging over the different $z$'s, to the extent that they appear damped at longer times. Note, however, that all curves in Fig. 2(b) have practically saturated at their new equilibrium values prior to the appearance of oscillations.

We stress that no explicit damping factor was utilized in Fig. 2. A nonzero $\alpha$ depresses the oscillations in $n_d(t)$, which saturates at the new steady-state values indicated by arrows in Fig. 2(a). The difference $\delta n_d$ between the new equilibrium occupancy of $\mathcal{H}^f$ and the steady-state value reached serves as a sharp criterion for the accuracy of the TD-NRG. The smaller $\delta n_d$ is the better the TD-NRG performs on all time scales. This provides one with a valuable estimate for the accuracy of the TD-NRG in cases where no other reference exists.

*Single impurity Anderson model.*—The first nontrivial model which lacks an exact solution out of equilibrium is the SIAM, describing a spinful resonant level with an on-site repulsion $U$ :

$$\mathcal{H} = \sum_{k,\sigma} \varepsilon_{k\sigma} c_{k\sigma}^\dagger c_{k\sigma} + \sum_{\sigma=\pm 1} \left[ E_d(t) - \frac{\sigma}{2} H(t) \right] d_\sigma^\dagger d_\sigma + U \hat{n}_\uparrow^d \hat{n}_\downarrow^d + V(t) \sum_{k,\sigma} \{ d_\sigma^\dagger c_{k\sigma} + c_{k\sigma}^\dagger d_\sigma \}. \quad (7)$$

Here $\hat{n}_\sigma^d = d_\sigma^\dagger d_\sigma$. This Hamiltonian is commonly used to model a single Coulomb-blockade resonance in ultrasmall quantum dots. To probe the relaxation both in the spin and charge sectors, we consider in the following a simultaneous stepwise change in the energy of the level, $E_d(t) = \theta(-t) E_d^0 + \theta(t) E_d^1$, and in the local magnetic field, $H(t) = \theta(-t) H_0 + \theta(t) H_1$. We also permit a sudden change in the hybridization width $\Gamma(t) = \pi \rho_0 V^2(t)$: $\Gamma(t) = \theta(-t)\Gamma_0 + \theta(t)\Gamma_1$. As our prime interest is in the relaxation to a new Kondo state, we focus hereafter on $H_1 = 0$ and only briefly comment on nonzero $H_1$.

In the spirit of the experiment of Elzerman *et al.* [3] (which, however, did not sample the Kondo regime of interest here), we begin with a spin-polarized impurity, where the lower spin state is degenerate with the empty-orbital state: $E_d^0 - H_0/2 = 0$. At $t = 0$, both the local magnetic field is switched off and the energy of the level is shifted to $E_d^1 = -U/2$. The resulting time evolutions of the impurity occupancy $n_d(t) = \langle \hat{n}_\uparrow^d + \hat{n}_\downarrow^d \rangle(t)$ and magnetization $S_z(t) = \frac{1}{2} \langle \hat{n}_\uparrow^d - \hat{n}_\downarrow^d \rangle(t)$ are plotted in Fig. 3, for $T \to 0$, $H_0 = \Gamma_1$, and different values of $U$. Two separate initial conditions are considered: $\Gamma_0 = \Gamma_1$ and $\Gamma_0 = 0$, representing different relaxations to the strong-coupling fixed point. The former corresponds to relaxation from a spin-polarized mixed-valent state, while the latter describes evolution from a free-impurity fixed point.

Two distinct time scales are clearly visible in Fig. 3 for the relaxation of spin and charge. Similar to the RLM, $n_d(t)$ equilibrates on a time scale $t_{\rm ch} \propto 1/\Gamma_1$, and develops Rabi-type oscillations for $|E_d^1| > \Gamma_1$. For $t \gg t_{\rm ch}$, the occupancy must saturate at its new equilibrium value $n_d = 1$. This behavior is well captured by the TD-NRG, attesting to its accuracy. The long-time deviations $\delta n_d$ are less than 0.04 for $\Gamma_0 = \Gamma_1$ and less than 0.065 for $\Gamma_0 = 0$. Importantly, $\delta n_d$ is notably smaller for the SIAM than for the RLM with comparable $E_d^1$.

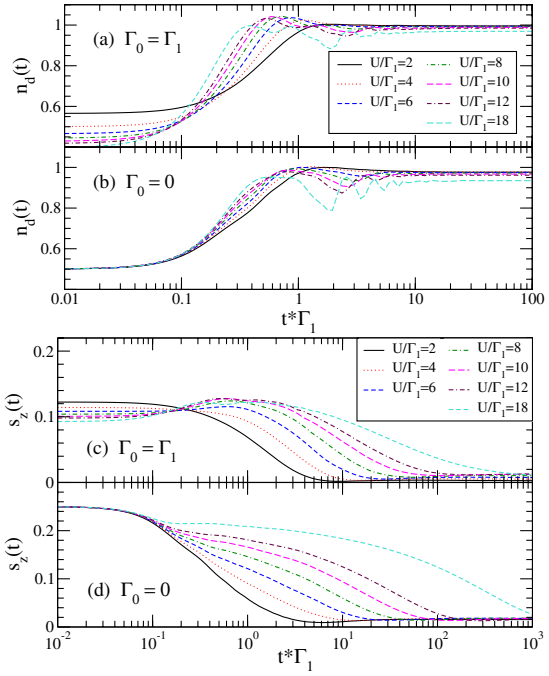


FIG. 3 (color online). Time-dependent occupancy $n_d(t)$, (a),(b) and magnetization $S_z(t)$, (c),(d) of the SIAM with $T \to 0$, $D/\Gamma_1 = 20$, $H_0 = 2E_d^0 = \Gamma_1$, $H_1 = 0$, $E_d^1 = -U/2$, and seven different values of $U/\Gamma_1 = 2, 4, 6, 8, 10, 12, 18$. Here $\Gamma_0 = \Gamma_1$ in (a) and (c), whereas $\Gamma_0 = 0$ in (b) and (d). NRG parameters: $\Lambda = 1.5$, $N_s = 1000$, $N_z = 16$, and $\alpha = 0.1$.

Contrary to $n_d(t)$, the spin magnetization $S_z(t)$ equilibrates on a much longer time scale $t_{\rm sp}$. To elucidate the strong $U$ dependence of $t_{\rm sp}$, we replotted the magnetization curves of Fig. 3 versus $t/t_K$ with $t_K = 1/T_K$, see Fig. 4. Here $T_K$ is the Kondo temperature of $\mathcal{H}^f$, defined by $T_K\chi(T_K) = 0.07$ [16] ($\chi$ being the impurity susceptibility of $\mathcal{H}^f$). While the initial dynamics of $S_z(t)$ is governed by $t_{\rm ch} \propto 1/\Gamma_1$, the eventual relaxation is clearly governed for $\Gamma_0 = 0$ by the Kondo time scale: $t_{\rm sp} \propto 1/T_K$ [17]. Indeed, all curves gradually collapse in Fig. 4(b) onto a single master curve, provided a stable local moment was formed on the level. By contrast, there is no universality in $t/t_K$ for $\Gamma_0 = \Gamma_1$. In fact, $S_z(t)$ differs in form from that of $\Gamma_0 = 0$, revealing a qualitative difference in the spin relaxation of an initially free impurity and an initially coupled one. A nonzero $H_1$ suppresses the Kondo effect. Accordingly, the spin relaxation time $t_{\rm sp}$ is reduced, approaching $t_{\rm ch}$ for $H_1 \gg T_K$ (not shown).

*Summary and discussion.*—A powerful new approach to the nonequilibrium dynamics of QIS was presented based upon Wilson's NRG. All states of the Wilson chain are summed over in this scheme, and no basis set reduction is imposed. We established the accuracy of the approach on all time scales by comparison to the exact solution of the RLM, and demonstrated its ability to access exceedingly long time scales by investigating the equilibration of the SIAM. Starting from a free impurity, the spin relaxation

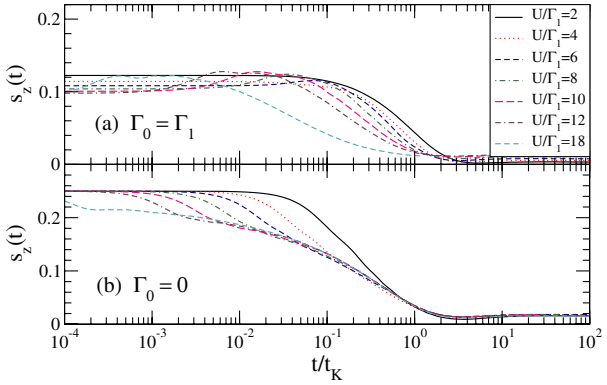


FIG. 4 (color online). The impurity magnetization curves of Fig. 3, replotted versus $t/t_K$ with $t_K = 1/T_K$. Here $\Gamma_0 = \Gamma_1$ in (a), while $\Gamma_0 = 0$ in (b).

time $t_{\rm sp}$ of the SIAM was shown to be governed by the Kondo time scale $t_K = 1/T_K$, for $T \ll T_K$. However, there is no universality in $t/t_K$. Spin relaxation is sensitive to the initial conditions imposed on the system. Although our specific examples were focused on Fermionic baths, the TD-NRG can equally be applied to bosonic baths [18]. This should allow for an accurate investigation of the time evolution of a two-level system [1] as relevant to quantum computers, and of biological donor-acceptor molecules.

We have benefited from discussions with R. Bulla, G. Czycholl, S. Kehrein, K. Ingersent, D. Vollhardt, M. Vojta, and especially E. Lebanon. F. B. A. acknowledges funding of the NIC, Forschungszentrum Jülich, under Project No. HHB000. A. S. was supported in part by the Centers of Excellence Program of the Israel Science Foundation.

[1] A. J. Leggett *et al.*, Rev. Mod. Phys. **59**, 1 (1987).
[2] M. A. Kastner, Rev. Mod. Phys. **64**, 849 (1992).
[3] J. M. Elzerman *et al.*, Nature (London) **430**, 431 (2004).
[4] L. V. Keldysh, Sov. Phys. JETP **20**, 1018 (1965).
[5] M. A. Cazalilla and J. B. Marston, Phys. Rev. Lett. **88**, 256403 (2002).
[6] A. J. Daley *et al.*, J. Stat. Mech. (2004) P04005.
[7] S. R. White and A. E. Feiguin, Phys. Rev. Lett. **93**, 076401 (2004).
[8] D. Gobert *et al.*, Phys. Rev. E **71**, 036102 (2005).
[9] P. Nordlander *et al.*, Phys. Rev. Lett. **83**, 808 (1999).
[10] K. G. Wilson, Rev. Mod. Phys. **47**, 773 (1975).
[11] T. A. Costi, Phys. Rev. B **55**, 3003 (1997).
[12] R. P. Feynman, *Statistical Mechanics, A Set of Lectures* (Benjamin, Reading, MA, 1972).
[13] W. Hofstetter, Phys. Rev. Lett. **85**, 1508 (2000).
[14] M. Yoshida *et al.*, Phys. Rev. B **41**, 9403 (1990).
[15] Details will be published elsewhere.
[16] H. R. Krishna-murthy, J. W. Wilkins, and K. G. Wilson, Phys. Rev. B **21**, 1003 (1980).
[17] D. Lobaskin and S. Kehrein, Phys. Rev. B **71**, 193303 (2005).
[18] R. Bulla *et al.*, Phys. Rev. Lett. **91**, 170601 (2003).